ASIAN JOURNAL OF CIVIL ENGINEERING (BHRC) VOL. 15, NO. 1 (2014)
PAGES 23-40

A NEW 3D HYDROGRADIENT TEST INSTRUMENT

A. Robati* and Gh. Barani
Department of Civil Engineering, College of Engineering, Shahid Bahonar University, Kerman, Iran

Received: 19 May 2012; **Accepted:** 10 May 2013

ABSTRACT

The purpose of this study is to design and construct an instrument for assessing three-dimensional hydraulic gradients based on the hydrogradient mathematical model in porous media. In order to properly investigate flow in porous media, three-dimensional details must be taken into consideration. Therefore, Mohr cyclides, which can be presented in three dimensions, are used and a beneficial instrument is designed and constructed based on the non-collinearity of the flow vector q and gradient vector J .

The cyclide surface is a geometric locus for all possible states of flow movement in a porous media field; depending on the field's hydraulic gradient components, in which one of these flow movements will occur. By specifying the values of the hydraulic gradient components, the flow direction will be assigned.

Keywords: Porous media; hydrogradient mathematical model; hydraulic gradient; cyclide; mohr diagram.

1. INTRODUCTION

Underground flow analysis is greatly impacted by the specified flow direction and porous media conditions present at the beginning of movement. The beginning of underground flow through porous media requires numerous conditions, such as securing a three-dimensional hydraulic gradient and a structurally stable matrix such that flow can pass through porous media with an erosion quantity suitable for an easy fluid flow (severe erosion can stop the flow of fluid by solid particles).

Darcy's law is a powerful experimental tool and phenomenological equation used to model flow in porous media flow. The equation can be linked to a more fundamental micro-scale model of flow through the pores of porous materials.

* E-mail address of the corresponding author: ammirrr@yahoo.com (A. Robati)

In the actual complex pore geometries of granular materials, Darcy's law (macro-scale) is derived through upscaling the incompressible Navier-Stokes (micro-scale) equations [1]. Therefore, Darcy's experimental law has sufficient theoretical credibility for this study.

The hydraulic stability of flow in porous media has many applications and advantages, such as efficient undercutting of bank failures, water tunneling stability, flow stability in subterranean channels, soil slope stability, the tectonic consequences of fluid over pressure, and other similar phenomena.

Chu – Agor et al. (2009) developed an empirical sediment transport function to predict seepage and demonstrated that the base seepage criterion for their studies is: "the hydraulic gradient should be greater than the critical hydraulic gradient $i > i_{cr}$ on the streamline curve". They also noted that three-dimensional functions may be better able to represent undercut shapes in future [2].

Young – Jin shin et al. [3] developed a ground reaction curve for underwater tunnels with seepage forces and decomposed the hydraulic gradient into radial and tangential components, finding that the radial component is the effective portion of the hydraulic gradient. However, in realistic underwater tunnels, the three-dimensional hydraulic gradient is dominant.

Robati and Barani [4] developed a water surface profile model for subterranean channels. The researchers explained that water could stably penetrate a subterranean channel if the hydraulic gradient occurs between the saturated zones and channel water level.

Using a two-dimensional flow deformation coupled with an analysis program, Cho and Lee [5,6] presented a procedure for calculating the safety factor for an unsaturated slope suffering from rainfall infiltration. Mourgues and Cobbold [7] have demonstrated some of the effects of fluid overpressure and seepage forces in tectonics.

The three-dimensional hydraulic gradient is a main factor in numerous phenomena that are directly related to flow in porous media. The aforementioned studies considered a hydraulic gradient that was greater than the critical hydraulic gradient on a streamline curve in both a one-dimensional curvilinear coordinate axis and two-dimensional Cartesian coordinate axes. However, three-dimensional factors must be considered in a proper investigation of flow in porous media [5]. In the real world, a medium is mostly non-homogeneous and non-isotropic, leading the generalized Darcy's law to present a relationship between specific discharge components (q_x, q_y, q_z), the hydraulic gradients (J_x, J_y, J_z), and the hydraulic conductivity tensor [8]. The hydraulic conductivities have the properties of second-rank tensors. Mohr cyclides are used to seek an efficient representation technique for obtaining three-dimensional presentations.

Coelho and Passchier (2008) introduced the Mohr cyclides as a way to represent geological tensors three-dimensionally for the first time. The researchers used Mohr cyclides for stress, flow and deformation tensors [9, 10].

To properly investigate flow in porous media, three-dimensional details must be considered; therefore, Robati and Barani developed a hydrogradient mathematical model. The main purpose of this study is to design and construct an instrument to investigate three-dimensional hydraulic gradients based on this hydrogradient mathematical model in porous media.

2. HYDROGRADIENT MATHEMATICAL MODEL

Previous studies have used superficial three-dimensional models to present three-dimensional flows in porous media; however, these models are actually two-dimensional. Robati and Barani considered three-dimensional details and used non-spherical fourth-degree surfaces, or *cyclides*, as a mathematical model. A novel mathematical model is considered for the non-collinearity of the flow vector q and gradient vector J to provide an actual perspective for three-dimensional modeling. Cyclide parameters were shown to remain constant when the coordinate system translates with rotation and a single translation to another coordinate system. Therefore, cyclide parameters and the related novel mathematical presentation are independent of any applied rotation and can be interpreted as a Mohr diagram. This novel mathematical model is nominated *Hydrogradient mathematical model*.

Developing a mathematical presentation of hydraulic gradients in porous media is fundamental for improving the opinion of flow in porous media.

2.1 Anisotropic permeability

The permeability and hydraulic conductivity of the porous medium are shown to be second-rank tensors. Some brief comments regarding these tensors are discussed below.

For anisotropic media, the relationship between specific discharge vectors (q_x, q_y, q_z) and gradient vectors (J_x, J_y, J_z) can generally be written as

$$\begin{aligned} q_x &= k_{xx}J_x + k_{xy}J_y + k_{xz}J_z \\ q_y &= k_{yx}J_x + k_{yy}J_y + k_{yz}J_z \\ q_z &= k_{zx}J_x + k_{zy}J_y + k_{zz}J_z \end{aligned} \tag{1}$$

or, in the matrix form, as $\{q_i\} = [k_{ij}]\{J_j\} (i, j = 1,2,3 \text{ or } x, y, z)$

$$\begin{bmatrix} q_x \\ q_y \\ q_z \end{bmatrix} = \begin{bmatrix} k_{xx} & k_{xy} & k_{xz} \\ k_{yx} & k_{yy} & k_{yz} \\ k_{zx} & k_{zy} & k_{zz} \end{bmatrix} \begin{bmatrix} J_x \\ J_y \\ J_z \end{bmatrix} \tag{2}$$

Each component k_{ab} relates gradients in the b-direction to flux in the a-direction. For example, the flow q_x is the sum of specific discharges caused by J_x, J_y and J_z

The essence of porous media is independent of the selected coordinate axes. The Mohr circle was used to classify states that include the same essence but are located in different coordinate axes.

If the hydraulic conductivity components k_{ij} of a tensor K in an x_i coordinate system are given, then their components $k_{p'q'}$ in another $x_{p'}$ system can be obtained from x_i coordinates, such that

$$k_{p'q'} = k_{ij}.\alpha_{pi}.\alpha_{qj} \qquad i, j, p, q = 1,2,3 \tag{3}$$

where α_{mn} is the directional cosine between axes x_m, x_n, and the direction in space is specified by unit vector $\overrightarrow{1u}$; thus, $\alpha_{mn} = \cos(\overrightarrow{1x_m}, \overrightarrow{1x_n})$.

In matrix notation, three-dimensional cases with direction cosines l, m, n between the new coordinate axes x', y', z' and the original coordinate axes x, y, z are defined as follows:

$$T = \begin{bmatrix} l_1 & m_1 & n_1 \\ l_2 & m_2 & n_2 \\ l_3 & m_3 & n_3 \end{bmatrix}$$

and

$$k_{i'j'} = T_{ij} k_{ij} T_{ij}^T \tag{4}$$

Thus, the matrices

$$\begin{bmatrix} k_{x'x'} & k_{x'y'} & k_{x'z'} \\ k_{y'x'} & k_{y'y'} & k_{y'z'} \\ k_{z'x'} & k_{z'y'} & k_{z'z'} \end{bmatrix} and \begin{bmatrix} k_{xx} & k_{xy} & k_{xz} \\ k_{yx} & k_{yy} & k_{yz} \\ k_{zx} & k_{zy} & k_{zz} \end{bmatrix},$$

have the same essence for a porous medium in different coordinate axes $(x'y', z')$ and (x, y, z).

A tensor or one set of k_{ij} can be calculated for any coordinate axis. Any set of k_{ij} shows tensor K in one coordinate axis, that one of them has the following diagonal form:

$$k_{i'j'} = \begin{bmatrix} k_{11} & 0 & 0 \\ 0 & k_{22} & 0 \\ 0 & 0 & k_{33} \end{bmatrix} \tag{5}$$

In this form, the three orthogonal axes are called principal axes, and $k_{11,}k_{22}, k_{33}$ are the eigenvalues or roots of the characteristic equation.

The characteristic equation is as follows [8]:

$$\begin{vmatrix} (k_{xx} - k) & k_{xy} & k_{xz} \\ k_{yx} & (k_{yy} - k) & k_{yz} \\ k_{zx} & k_{zy} & (k_{zz} - k) \end{vmatrix} = 0$$

$$k^3-(k_{xx}+k_{yy}+k_{zz})k^2+(k_{xx}k_{yy}+k_{yy}k_{zz}+k_{zz}k_{xx}-k_{xy}^2-k_{yz}^2-k_{zx}^2)k-(k_{xx}k_{yy}k_{zz}+2k_{xy}k_{yz}k_{zx} -k_{xx}k_{yz}^2-k_{yy}k_{zx}^2-k_{zz}k_{xy}^2)=0 \quad (6)$$

under the following assumptions:

$$\begin{aligned} k_{xy} &= k_{yx} \\ k_{xz} &= k_{zx} \\ k_{yz} &= k_{zy} \end{aligned} \quad (7)$$

In any coordinate system, the characteristic equation that is defined for one porous medium is based on an axis of infinite coordinate systems and has the same form, roots and principal valves (K_{11}, K_{22} and k_{33}).

Furthermore, in mathematical form any root e_i of this equation one eigenvalue (e_1, e_2, e_3).

2.2 Previous restricted consideration for flow in porous media

Although three-dimensional details must be considered when investigating flow in porous media, porous media properties have thus far been restricted to two-dimensional cases with specific interpretations for simplification.

Most porous media conditions are restricted to the case of two equal hydraulic conductivities, or $k_{xx}=k_{yy}\neq k_{zz}$, where *x, y and z* are principal directions. In this case, any direction in the *xy* plane can be considered the principal direction. Media with numerous thin layers and alternating permeability exhibit this property [8].

In an isotropic medium where $k_{xx}=k_{yy}=k_{zz}=k$, any direction can be considered the principal direction, and the relationships between the components of vectors q and J take the following forms:

$$\begin{aligned} q &= k_{xx}.J_x \\ q &= k_{yy}.J_y \\ q &= k_{zz}.J_z \end{aligned} \quad (8)$$

For two-dimensional flow in the *xy* plane, $\frac{\partial(-)}{\partial z}=0$ at any point, where "(−)" refers to any flow property in porous media. For a three-dimensional flow through an isotropic medium, this requirement leads to the conclusion that both J_z and q_z must always be zero. In general, when the medium is anisotropic, the condition $J_z=0$ does not necessarily mean that $q_z=0$, because in this case, the q_z contributions from J_x and J_y are efficient, such

that $q_z = k_{zx}J_x + k_{zy}J_y$

Thus, a two-dimensional flow is possible when $k_{zx} = k_{zy} = k_{xz} = k_{yz} = 0$ or more generally when $k_{zx}J_x + k_{zy}J_y = 0$. If one component of J vanishes when x, y *and* z are the principal directions, it is sufficient to produce a two-dimensional flow in planes that are normal to the direction of the vanished component.

Therefore, a two-dimensional flow is a very specific state due to its restrictions, whereas flow in porous media includes three-dimensional details.

Previous studies have simplified three-dimensional flow in porous media in two-dimensional base flows: the *plane flow* and the *plane gradient* (this nomination is done by authors).

In the *plane flow* case, the flow is in a narrow and relatively long sand-packed column; the channel flow compels the fluid to move in a certain direction in the longitudinal of channel flow q. In the *plane gradient* case, the flow is in a very wide and relatively thin porous medium between two parallel equipotential plane boundaries. The gradient is almost parallel to the normal of both planes, and the fluid will move in the direction of least resistance, or the gradient direction J. In the *plane flow* case, the flow is forced to move in a certain direction q, while in the *plane gradient* case, fluid is free to choose the path of least resistance and highest permeability (gradient direction J).

In an anisotropic real medium, the vectors q and J are collinear if and only if they coincide on the principal axes direction.

2.3 Cyclides and their properties

A general cyclide is a non-spherical fourth-degree surface, introduced by Dupin (1822), which can be defined in canonical form by an implicit equation as follows [10,11]:

$$(x^2 + y^2 + z^2 - D^2 + B^2)^2 = 4(Ax - CD)^2 + 4(By)^2 \tag{9}$$

where A, B, C and D are constant parameters, and $B^2 = A^2 - C^2$. In a sample case with two positive constants A and $C(C < A)$, the shape of the Dupin cyclide $Z(A, C, D)$ is shown in Figure 1. The longitudinal principal circles have centers at $(\pm A, 0, 0)$, and their radii are $D \mp C$, Ref. [12].

$$x = \frac{B\sin\psi(C\cos\theta - D)}{A - C\cos\theta\cos\psi}$$

$$y = \frac{D(C - A\cos\theta\cos\psi) + B^2\cos\theta}{A - C\cos\theta\cos\psi} \quad \text{with} \begin{cases} \theta \geq 0 \\ \psi \leq 180 \end{cases} \tag{10}$$

$$z = \frac{B\sin\theta(A - D\cos\psi)}{A - C\cos\theta\cos\psi}$$

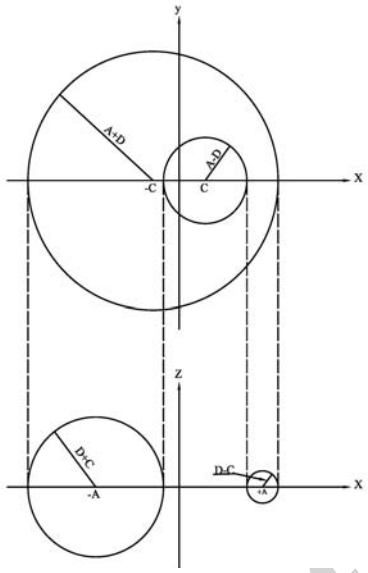

Figure 1. Longitudinal and latitudinal principal circles of the Dupin cyclide [12]

A cyclide can also be defined in the parametric system for a general point (θ,ψ) Pratt [13].

The relative magnitude of parameters A,C and $D(B$ is always dependent$)$ define the shape of the surface for the cyclide family shown in table 1 by Shene [12].

The cyclide properties are as follows [5, 12]:

1) All lines in the curvature of the cyclide that are defined by equal values of θ or ψ are circles.

2) The cyclide has two orthogonal planes of symmetry.

3) The cyclide is fully defined by four major circles (two in each symmetry plane) that are given by the following parameters:

$\theta = 0, \theta = 180, \psi = 0, \psi = 180$. If parameter D is equal to either A or C, three circles are sufficient.

4) The radii of the major circles are defined by A,C and D.

2.4 Mohr cyclides for porous media

Any hydraulic conductivity tensor relates vectors q and J as follows:

$$q_i = k_{ij}.J_j \tag{11}$$

This equation can be expanded to

$$\begin{aligned} q_x &= k_{xx}J_x + k_{xy}J_y + k_{xz}J_z \\ q_y &= k_{yx}J_x + k_{yy}J_y + k_{yz}J_z \\ q_z &= k_{zx}J_x + k_{zy}J_y + k_{zz}J_z \end{aligned} \tag{12}$$

To present the hydrogradient model of flow in porous media, the Mohr cyclides are defined by the properties of J, including its magnitude $\bar{J} = (J_x^2 + J_y^2 + J_z^2)^{\frac{1}{2}}$ and orientation in space. For Mohr cyclide purposes, only two angles (φ and δ) are necessary.

The definition of φ can be defined as the angle between J and q and is given by the dot product.

$$\cos\varphi = \frac{J_x q_x + J_y q_y + J_z q_z}{\bar{J}.\bar{q}} \tag{13}$$

The definition of δ is less intuitive. First, a third vector, U, must be introduced as the pole of the plane defined by J and q. The components of U can be obtained with the cross product of J and q.

$$J \times q = \det\begin{bmatrix} u_x & u_y & u_z \\ J_x & J_y & J_z \\ q_x & q_y & q_z \end{bmatrix} \tag{14}$$

where

$$\begin{aligned} u_x &= J_y q_z - J_z q_y \\ u_y &= J_z q_x - J_x q_z \\ u_z &= J_x q_y - J_y q_x \end{aligned} \tag{15}$$

δ is the angle between U and e, one of the eigenvectors of k_{ij}. Any of the eigenvectors can be chosen, depending on the eigenvalues of the characteristic equation. However, the chosen eigenvector must be an eigenvector of k_{ij}, as opposed to any other tensor defined with, by or through k_{ij}, unless they are identical. Failure to respect this rule results in useless graphs of undetermined geometrical pedigree.

Then, δ can be calculated as follows:

$$\cos\delta = \frac{u_x e_x + u_y e_y + u_z e_z}{\bar{u}.\bar{e}} \tag{16}$$

where $\bar{e}$ is the corresponding eigenvalue.

Subsequently, the Mohr cyclide for k_{ij} can be plotted with the following polar coordinates:

$$X_m = \bar{J}\sin\varphi\cos\delta$$
$$Y_m = \bar{J}\cos\varphi \qquad (17)$$
$$Z_m = \bar{J}\sin\varphi\sin\delta$$

Table 1: the cyclide family classified based on parameters A, C and D. The black lines represent the principal circles of each cyclide. All of the lines in the curvature of the cyclide defined by equal values of θ or ψ are circles [10].

Parameters	**Cyclide type**	**shape**
$0 < D \le C \le A$	Double-crescent Cyclide	
$D = C$	Single-crescent Cyclide	
$0 \le C < D \le A$	Ring cyclide (torus)	
$D = A$	Torus with converging point or single singularity spindle-cyclide	
$0 \le C \le A < D$	Double-singularity spindle-cyclide	

When assigning the surface of a cyclide family, it is useful to note that the cyclide discussion is based on monoclinic or higher tensor symmetry, characterized by at least one eigenvector parallel to one of the axes of the reference frame. This condition imposes some restrictions on the component of k_{ij} , which can be written in the following three ways [10]:

$$\text{a)}\quad k_{ij}=\begin{bmatrix} a & b & 0\\ c & d & 0\\ 0 & 0 & f\end{bmatrix} \qquad \text{b)}\quad k_{ij}=\begin{bmatrix} a & 0 & b\\ 0 & f & 0\\ c & 0 & d\end{bmatrix} \qquad \text{c)}\quad k_{ij}=\begin{bmatrix} f & 0 & 0\\ 0 & a & b\\ 0 & c & d\end{bmatrix} \tag{18}$$

For simplification, small letters are used instead of the typical tensor components k_{ij} .The type of surface described by the tensor depends on the actual parameters used to define the analytical forms. The Mohr cyclide shape can be predicted by assessing the component's relative magnitudes, particularly f , which corresponds to the eigenvalue of the eigenvector e used to define θ as follows [10]:

I) If $f > a,d$, then the Mohr cyclide is a positive single-crescent cyclide;

II) If $f < a,d$, then the Mohr cyclide is a negative single-crescent cyclide;

III) If $a,b < f < a,d$, then the Mohr cyclide is a torus.

Each of these surfaces has a converging point at f and intersects the Y_m Mohr coordinate axis at the points given by the eigenvalues of k_{ij}

A,B,C and D can now be defined using the equations in table 2. Substituting these values in the parametric equation (16) for any point (θ,ψ) produces a system of equations that defines a surface of the cyclide family as follows [10]:

$$\begin{aligned} x_{m'} &= \frac{B\sin\psi(C\cos\theta - D)}{A - C\cos\theta\cos\psi}\\ y_{m'} &= \frac{D(C - A\cos\theta\cos\psi) + B^2\cos\theta}{A - C\cos\theta\cos\psi} \quad \text{with} \begin{cases} \theta \geq 0\\ \psi \leq 180\end{cases}\\ z_{m'} &= \frac{B\sin\theta(A - D\cos\psi)}{A - C\cos\theta\cos\psi}\end{aligned} \tag{19}$$

The system of equations (19) defines a surface of the cyclide family; however, it does not define the Mohr cyclide for k_{ij} because it does not account for some of the Mohr cyclide's properties. This defect can be resolved by introducing an angle ρ to address the eventual tensor asymmetry. ρ is the angle between the negative Y_m Mohr coordinate and the cyclide vertical symmetry plane and is expressed as follows:

$$\begin{aligned} \tan\rho &= \frac{c-b}{a+d+2f} \quad \text{if} \quad f > E_y\\ &\text{or}\\ \tan\rho &= \frac{c-b}{a+d+2f} \quad \text{if} \quad f < E_y\end{aligned} \tag{20}$$

The parametric Mohr cyclide can be obtained by the multiplying the coordinates given in (19) by the rotation matrix T_{ij} and the single translate in X_m, Y_m plane of the Mohr coordinate axes as follows:

$$\begin{bmatrix} x_m \\ y_m \\ z_m \end{bmatrix} = \begin{bmatrix} \cos\rho & -\sin\rho & 0 \\ \sin\rho & \cos\rho & 0 \\ 0 & 0 & 1 \end{bmatrix} \begin{bmatrix} x_{m'} \\ y_{m'} \\ z_{m'} \end{bmatrix} + \begin{bmatrix} E_x \\ E_y \\ 0 \end{bmatrix} \tag{21}$$

Rotation translate
Then,

$$\begin{aligned} x_m &= x_{m'}\cos\rho - y_{m'}\sin\rho + E_x \\ y_m &= x_{m'}\sin\rho - y_{m'}\cos\rho + E_y \\ z_m &= z_{m'} \end{aligned} \tag{22}$$

Table 2: Parameters of the Mohr cyclide [10]

Parameter		$f > a,d$	$f < a,d$	$a,b < f < a,d$
		Positive single-crescent	*Negative single-crescent*	*Torus with converging point*
A		$\sqrt{(E_y - f)^2 + E_x^2}$	$\sqrt{(E_y - f)^2 + E_x^2}$	$\sqrt{(\frac{(b+c)^2 + (a-d)^2}{4}}$
B		$\sqrt{A^2 - C^2}$	$\sqrt{A^2 - C^2}$	$\sqrt{A^2 - C^2}$
C		$\sqrt{(\frac{(b+c)^2 + (a-d)^2}{4}}$	$\sqrt{(\frac{(b+c)^2 + (a-d)^2}{4}}$	$\sqrt{(E_y - f)^2 + E_x^2}$
D		C	C	A
E	E_x	$\frac{c-b}{2}$	$\frac{c-b}{2}$	$\frac{c-b}{2}$
	E_y	$\frac{a+d+2f}{4}$	$\frac{a+d+2f}{4}$	$\frac{a+d+2f}{4}$

A cyclide can be a Mohr diagram for the k_{ij} tensor because its parameters A, B, C, D, E

and ρ remain constant when any combination of the components is chosen from the infinite possibilities available for defining k_{ij}. Equivalently, the Mohr cyclide for k_{ij} is identical to the Mohr cyclide for $k_{i'j'}$ [10].

2.5 Numerical example of the hydrogradient mathematical model

Based on Robati and Barani's study, flow in porous media can be presented by the cyclide surface, and cyclide parameters are independent from any applied rotation. Thus, this presentation can be interpreted as a Mohr diagram.

One porous medium containing the following hydraulic permeability with related flow and gradient vectors could be shown by the hydrogradient presentation in the following form Figure 2.

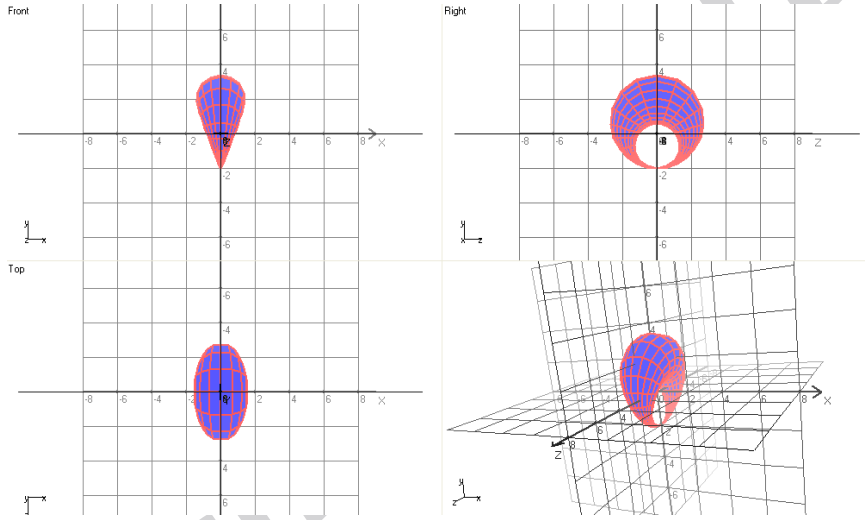

Figure 2. Hydrogradient mathematical presentation sample

$$(k_{xx} = 0.00002, k_{xy} = 0.00001, k_{xz} = 0, k_{yx} = 0.00001,$$
$$k_{yy} = 0.00003, k_{yz} = 0, k_{zx} = 0, k_{zy} = 0, k_{zz} = 0.00005)$$

To assign flow in this example, adjusting the coordinate axis is sufficient. By changing axes x, y, z to J_x, J_y, J_z and specifying the values of J_x, J_y, J_z, the flow direction can be assigned for linked porous media. The described cyclide is a geometric locus for all possible states of flow movement in porous media field; depending on the components of the hydraulic gradient, one of these states of flow movement will occur.

3. SCOPE

In real porous media, when three-dimensional hydraulic gradients affect the porous medium, the flow starts to move in special direction. Introducing special coordinate axes that coincide

with this flow pattern causes the hydraulic conductivity tensor to take on a special form. This tensor can be presented by cyclide as Mohr diagram. The Mohr cyclides are geometric locus for all possible states of flow movement in porous media fields that consider non-collinearity of the flow vector q and gradient vector J . Depending on the components of the hydraulic gradient, one of these states of flow movement will occur. By specifying the values of the hydraulic gradient components, the related state can be assigned. Thus designing and construction of an instrument for measuring hydraulic gradient components, is very advantageous.

4. INSTRUMENT DESIGN

Based on Robati and Barani's study, flow in porous media can be presented by the cyclide surface that cyclide parameters are independent of any applied rotation. Thus, this presentation can be interpreted as a Mohr diagram and can be used to depict one porous medium containing the special hydraulic permeability with the related flow and gradient vectors.

An instrument is designed and constructed to specify the values of the hydraulic gradient components based on the three-dimensional hydrogradient mathematical presentation. The design of each part of the instrument includes the criteria, which must consider the related purposes and solutions of their predominant difficulties. The instrument is composed of many parts; each of them has its own criteria and related properties. The designed instrument includes four essential parts: the three-dimensional hydraulic gradient exertion case, the hydraulic gradient creative tanks, the piezometer board and the control system.

4.1 Designing of three-dimensional hydraulic gradient exertion case

The three-dimensional hydraulic gradient exertion case is made of Plexiglas, in which three-dimensional hydraulic gradients affect the porous medium. Creating a region in porous media under the three hydraulic gradient components in any direction of the coordinate axes refers to allow a region in which the shortest length of streamline in any direction of flow is equal to another streamline that coincides in the other direction of flow.

By regarding this point in design of the exertion case, a region under the pure hydraulic gradient can be developed.

Finally by constructing and testing several models, the optimal model is selected; this model is presented in Figure 3.

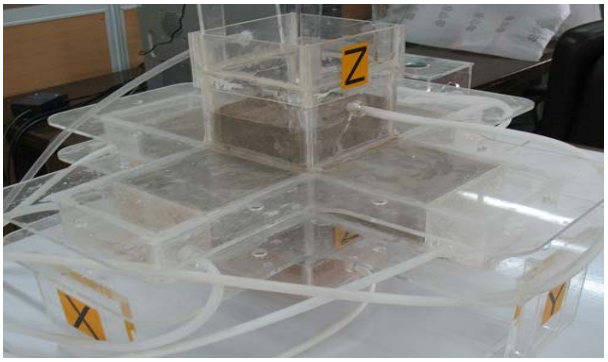

Figure 3. Picture of the three-dimensional hydraulic gradient exertion case

4.2 Designing of The hydraulic gradient creative tanks

The hydraulic gradient creative tanks include five elevated tanks; four of these tanks have the same design, and the other one has a different design. Each couple of tanks of the first group creates hydraulic gradients in the x and y directions, and the last tank creates a hydraulic gradient in the z direction by coupling with the top reservoir in the exertion case. The hydraulic gradients of the creative tanks in the x and y directions are discrete but the hydraulic gradient in the tank in the z direction is continuous. The discrete or continuous nature of the hydraulic gradient refers to the way in which the hydraulic gradient is exerted on the porous medium. In this instrument, for the x and y directions, the amount of hydraulic potential head located upstream or downstream of the exertion case varies step by step but in the z direction, the hydraulic potential head located upstream varies continuously (Figure 4).

Figure 4. Picture of the hydraulic gradient creative tanks

4.3 Designing of The piezometer board

The piezometer board is an indicator of the hydraulic potential head that are located at the upstream and downstream of the exertion case in any direction (x, y or z).The piezometer head can be assessing if it is measured just at the beginning and end of the exertion case in the x, y and z directions. The piezometer board is shown in Figure 5.

Figure 5. Piezometer board

4.4. Designing of The control system

The control system controls the fluid level in the fifth *hydraulic gradient creative tank* by turning the electric valve connected to it either on or off.

Determining when to turn the valves on or off is an important issue, which is solved by using a control system. This system accepts a video stream as an input and analyzes it to find changes in the sequence of images. If changes occur by flow movements, then the valves will be shut off via a command, which is sent to a switch. The flowchart and a simplified schematic of this system are shown in Figures 6. and 7., respectively.

The fluid flow detection system contains software and hardware. The hardware consists of three parts: the camera, switch, and electrical valves. The software detects changes in the sequence of images that was received from the camera. The camera is aligned on the surface of the fluid on the top of the *hydraulic gradient exertion case* to detect changes by the flow movements. If any change is detected, a shut off command is sent to the valves via the parallel port of the computer to the switches. The output signal of the parallel port will turn the valves on or off via a transistor which acts as an amplifier and a magnetic relay which acts as a switch. After the valves are shut off, the height of the fluid in the tank can be

measured.

5. CONCLUSION

Based on the *hydrogradient mathematical model in porous media*, the *3D hydrogradient test instrument* was designed and constructed to investigate three-dimensional hydraulic gradients. This instrument was tested and can be used to measure hydraulic gradients in any Cartesian direction. This instrument is the first step in demonstrating the criteria for the movement of fluid flow in porous media. Future research will address the assigning of criteria to various porous media and hydraulic gradient compositions.

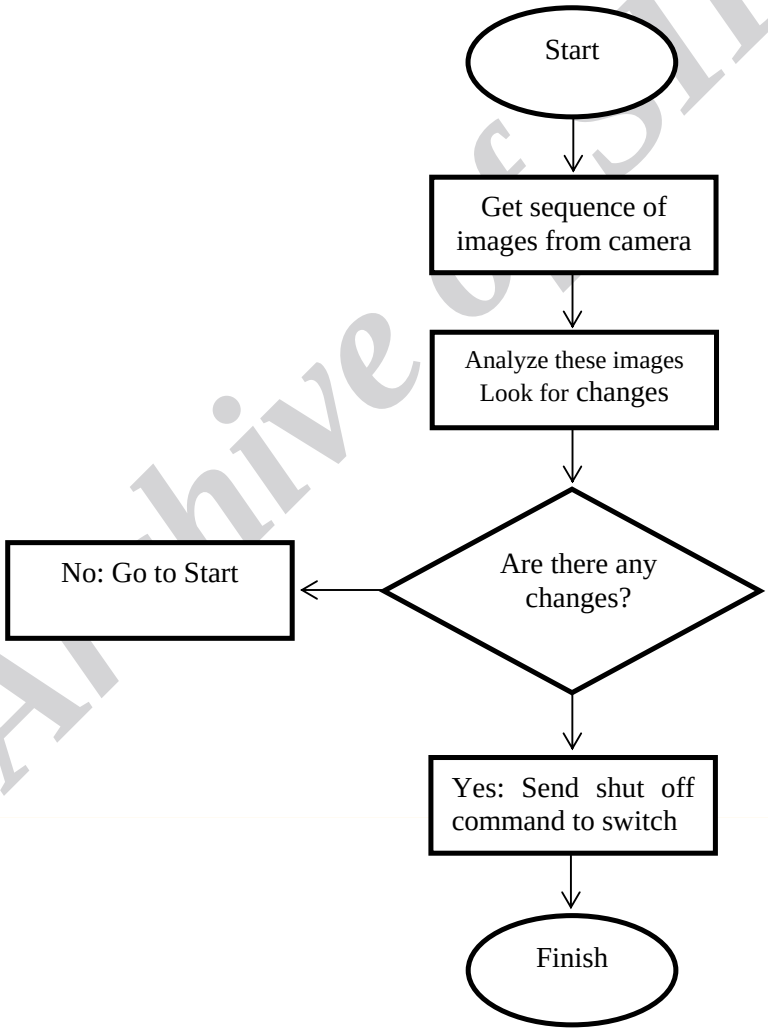

Figure 6. Flowchart of the control system

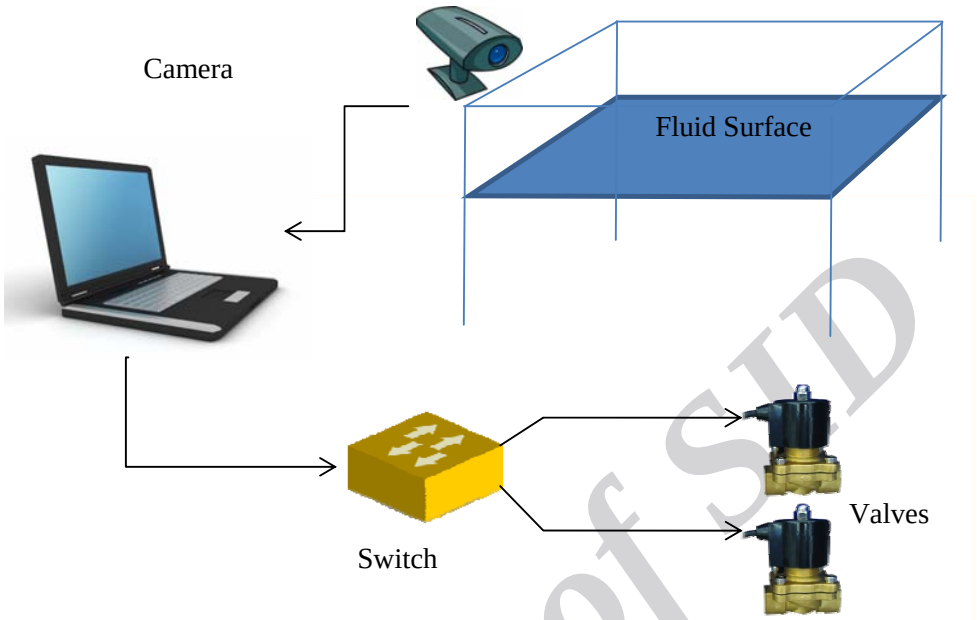

Figure 7. Parts of the fluid flow detection system

REFERENCES

1. Narsilio GA., Buzzi O, Fityus S, Yun TS, Smith DW. Up scaling of Navier–Stokes equation in porous media: Theoretical, numerical and experimental approach, *Computer and Geotechnics*, **36**(2009) 1200-6.
2. Chu–Agor ML, Fox GA, Wilson GV. Empirical sediment transport function predicting seepage erosion undercutting for cohesive bank failure prediction, *Journal of Hydrology*, **377**(2009) 155-64.
3. Shin YJ, Kim BM, Shin JH, Lee IM. The ground reaction curve of underwater tunnels considering seepage forces, *Tunneling and Underground Space Technology*, **25**(2010) 315-24.
4. Robati A, Barani Gh. Modeling of water surface profile in subterranean channel by differential quadrature Method (DQM), *Applied Mathematical Modeling*, **33**(2009) 1295-1305.
5. Allen S, Dutta D. Cyclides in pure blending I, *Computer Aided Geometric Design*, **14**(1997) 57-75.
6. Cho SE, Lee SR. Instability of unsaturated soil slopes due to infiltration, *Computer and Geotechnics*, **28**(2001) 185-208.
7. Mourgues R, Cobbold PR. Some tectonic consequences of fluid overpressures and seepage forces as demonstrated by sandbox modeling, *Tectonophysices*, **376**(2003) 75-

97.
8. Bear J. *Dynamics of fluids in porous Media*, Elsevier Publishing Company, United States of America, 1975, ISBN: 0-444-00114-x.
9. Coelho S, Passchier C, Mohr–cyclides. A 3D representation of geological tensors the examples of stress and flow, *Journal of Structural Geology*, **30**(2008) 580-601.
10. Coelho S. *Quantification Tools in Structural Geology Based in Field Examples form Namibia*, Ph.D. thesis, Department of Earth Science, University of Mainz, Mainz, Germany, 2007.
11. Dupin CP. *Application de Geometric et de Mechanique a La Marine*, aux ponts et chausses, etc. Bachelier, Paris, 1822.
12. Shene GK. Do blending and offsetting commute for Dupin cycilides, *Computer Aided Geometric Design*, **17**(2000) 891-910.
13. Pratt MJ. Cyclides in computer aided geometric design, *Computer Aided Geometric Design*, **7**(1990) 221-42.